August 2008

BaBar-PUB-08/002
SLAC-PUB-13249

arXiv:0805.4796v1 [hep-ex] 30 May 2008

A Measurement of *CP* Asymmetry in $b \to s\gamma$ using a Sum of Exclusive Final States

B. Aubert,[1] M. Bona,[1] Y. Karyotakis,[1] J. P. Lees,[1] V. Poireau,[1] X. Prudent,[1] V. Tisserand,[1] A. Zghiche,[1] J. Garra Tico,[2] E. Grauges,[2] L. Lopez,[3] A. Palano,[3] M. Pappagallo,[3] G. Eigen,[4] B. Stugu,[4] L. Sun,[4] G. S. Abrams,[5] M. Battaglia,[5] D. N. Brown,[5] J. Button-Shafer,[5] R. N. Cahn,[5] R. G. Jacobsen,[5] J. A. Kadyk,[5] L. T. Kerth,[5] Yu. G. Kolomensky,[5] G. Kukartsev,[5] G. Lynch,[5] I. L. Osipenkov,[5] M. T. Ronan,[5, *] K. Tackmann,[5] T. Tanabe,[5] W. A. Wenzel,[5] C. M. Hawkes,[6] N. Soni,[6] A. T. Watson,[6] H. Koch,[7] T. Schroeder,[7] D. Walker,[8] D. J. Asgeirsson,[9] T. Cuhadar-Donszelmann,[9] B. G. Fulsom,[9] C. Hearty,[9] T. S. Mattison,[9] J. A. McKenna,[9] M. Barrett,[10] A. Khan,[10] M. Saleem,[10] L. Teodorescu,[10] V. E. Blinov,[11] A. D. Bukin,[11] A. R. Buzykaev,[11] V. P. Druzhinin,[11] V. B. Golubev,[11] A. P. Onuchin,[11] S. I. Serednyakov,[11] Yu. I. Skovpen,[11] E. P. Solodov,[11] K. Yu. Todyshev,[11] M. Bondioli,[12] S. Curry,[12] I. Eschrich,[12] D. Kirkby,[12] A. J. Lankford,[12] P. Lund,[12] M. Mandelkern,[12] E. C. Martin,[12] D. P. Stoker,[12] S. Abachi,[13] C. Buchanan,[13] J. W. Gary,[14] F. Liu,[14] O. Long,[14] B. C. Shen,[14, *] G. M. Vitug,[14] Z. Yasin,[14] L. Zhang,[14] H. P. Paar,[15] S. Rahatlou,[15] V. Sharma,[15] C. Campagnari,[16] T. M. Hong,[16] D. Kovalskyi,[16] M. A. Mazur,[16] J. D. Richman,[16] T. W. Beck,[17] A. M. Eisner,[17] C. J. Flacco,[17] C. A. Heusch,[17] J. Kroseberg,[17] W. S. Lockman,[17] T. Schalk,[17] B. A. Schumm,[17] A. Seiden,[17] M. G. Wilson,[17] L. O. Winstrom,[17] E. Chen,[18] C. H. Cheng,[18] D. A. Doll,[18] B. Echenard,[18] F. Fang,[18] D. G. Hitlin,[18] I. Narsky,[18] T. Piatenko,[18] F. C. Porter,[18] R. Andreassen,[19] G. Mancinelli,[19] B. T. Meadows,[19] K. Mishra,[19] M. D. Sokoloff,[19] F. Blanc,[20] P. C. Bloom,[20] W. T. Ford,[20] J. F. Hirschauer,[20] A. Kreisel,[20] M. Nagel,[20] U. Nauenberg,[20] A. Olivas,[20] J. G. Smith,[20] K. A. Ulmer,[20] S. R. Wagner,[20] R. Ayad,[21, †] A. M. Gabareen,[21] A. Soffer,[21, ‡] W. H. Toki,[21] R. J. Wilson,[21] D. D. Altenburg,[22] E. Feltresi,[22] A. Hauke,[22] H. Jasper,[22] M. Karbach,[22] J. Merkel,[22] A. Petzold,[22] B. Spaan,[22] K. Wacker,[22] V. Klose,[23] M. J. Kobel,[23] H. M. Lacker,[23] W. F. Mader,[23] R. Nogowski,[23] J. Schubert,[23] K. R. Schubert,[23] R. Schwierz,[23] J. E. Sundermann,[23] A. Volk,[23] D. Bernard,[24] G. R. Bonneaud,[24] E. Latour,[24] Ch. Thiebaux,[24] M. Verderi,[24] P. J. Clark,[25] W. Gradl,[25] S. Playfer,[25] A. I. Robertson,[25] J. E. Watson,[25] M. Andreotti,[26] D. Bettoni,[26] C. Bozzi,[26] R. Calabrese,[26] A. Cecchi,[26] G. Cibinetto,[26] P. Franchini,[26] E. Luppi,[26] M. Negrini,[26] A. Petrella,[26] L. Piemontese,[26] E. Prencipe,[26] V. Santoro,[26] F. Anulli,[27] R. Baldini-Ferroli,[27] A. Calcaterra,[27] R. de Sangro,[27] G. Finocchiaro,[27] S. Pacetti,[27] P. Patteri,[27] I. M. Peruzzi,[27, §] M. Piccolo,[27] M. Rama,[27] A. Zallo,[27] A. Buzzo,[28] R. Contri,[28] M. Lo Vetere,[28] M. M. Macri,[28] M. R. Monge,[28] S. Passaggio,[28] C. Patrignani,[28] E. Robutti,[28] A. Santroni,[28] S. Tosi,[28] K. S. Chaisanguanthum,[29] M. Morii,[29] R. S. Dubitzky,[30] J. Marks,[30] S. Schenk,[30] U. Uwer,[30] D. J. Bard,[31] P. D. Dauncey,[31] J. A. Nash,[31] W. Panduro Vazquez,[31] M. Tibbetts,[31] P. K. Behera,[32] X. Chai,[32] M. J. Charles,[32] U. Mallik,[32] J. Cochran,[33] H. B. Crawley,[33] L. Dong,[33] V. Eyges,[33] W. T. Meyer,[33] S. Prell,[33] E. I. Rosenberg,[33] A. E. Rubin,[33] Y. Y. Gao,[34] A. V. Gritsan,[34] Z. J. Guo,[34] C. K. Lae,[34] A. G. Denig,[35] M. Fritsch,[35] G. Schott,[35] N. Arnaud,[36] J. Béquilleux,[36] A. D'Orazio,[36] M. Davier,[36] J. Firmino da Costa,[36] G. Grosdidier,[36] A. Höcker,[36] V. Lepeltier,[36] F. Le Diberder,[36] A. M. Lutz,[36] S. Pruvot,[36] P. Roudeau,[36] M. H. Schune,[36] J. Serrano,[36] V. Sordini,[36] A. Stocchi,[36] W. F. Wang,[36] G. Wormser,[36] D. J. Lange,[37] D. M. Wright,[37] I. Bingham,[38] J. P. Burke,[38] C. A. Chavez,[38] J. R. Fry,[38] E. Gabathuler,[38] R. Gamet,[38] D. E. Hutchcroft,[38] D. J. Payne,[38] C. Touramanis,[38] A. J. Bevan,[39] K. A. George,[39] F. Di Lodovico,[39] R. Sacco,[39] M. Sigamani,[39] G. Cowan,[40] H. U. Flaecher,[40] D. A. Hopkins,[40] S. Paramesvaran,[40] F. Salvatore,[40] A. C. Wren,[40] D. N. Brown,[41] C. L. Davis,[41] K. E. Alwyn,[42] N. R. Barlow,[42] R. J. Barlow,[42] Y. M. Chia,[42] C. L. Edgar,[42] G. D. Lafferty,[42] T. J. West,[42] J. I. Yi,[42] J. Anderson,[43] C. Chen,[43] A. Jawahery,[43] D. A. Roberts,[43] G. Simi,[43] J. M. Tuggle,[43] C. Dallapiccola,[44] S. S. Hertzbach,[44] X. Li,[44] E. Salvati,[44] S. Saremi,[44] R. Cowan,[45] D. Dujmic,[45] P. H. Fisher,[45] K. Koeneke,[45] G. Sciolla,[45] M. Spitznagel,[45] F. Taylor,[45] R. K. Yamamoto,[45] M. Zhao,[45] S. E. Mclachlin,[46, *] P. M. Patel,[46] S. H. Robertson,[46] A. Lazzaro,[47] V. Lombardo,[47] F. Palombo,[47] J. M. Bauer,[48] L. Cremaldi,[48] V. Eschenburg,[48] R. Godang,[48] R. Kroeger,[48] D. A. Sanders,[48] D. J. Summers,[48] H. W. Zhao,[48] S. Brunet,[49] D. Côté,[49] M. Simard,[49] P. Taras,[49] F. B. Viaud,[49] H. Nicholson,[50] G. De Nardo,[51] L. Lista,[51] D. Monorchio,[51] C. Sciacca,[51] M. A. Baak,[52] G. Raven,[52] H. L. Snoek,[52] C. P. Jessop,[53] K. J. Knoepfel,[53] J. M. LoSecco,[53] G. Benelli,[54] L. A. Corwin,[54] K. Honscheid,[54] H. Kagan,[54] R. Kass,[54] J. P. Morris,[54] A. M. Rahimi,[54] J. J. Regensburger,[54] S. J. Sekula,[54] Q. K. Wong,[54] N. L. Blount,[55] J. Brau,[55] R. Frey,[55] O. Igonkina,[55] J. A. Kolb,[55] M. Lu,[55] R. Rahmat,[55] N. B. Sinev,[55] D. Strom,[55] J. Strube,[55] E. Torrence,[55] G. Castelli,[56] N. Gagliardi,[56] A. Gaz,[56] M. Margoni,[56] M. Morandin,[56] M. Posocco,[56] M. Rotondo,[56] F. Simonetto,[56] R. Stroili,[56] C. Voci,[56] P. del Amo Sanchez,[57] E. Ben-Haim,[57] H. Briand,[57] G. Calderini,[57]

Published in the Physical Review Letters

Work supported in part by US Department of Energy contract DE-AC02-76SF00515

J. Chauveau,[57] P. David,[57] L. Del Buono,[57] O. Hamon,[57] Ph. Leruste,[57] J. Malclès,[57] J. Ocariz,[57] A. Perez,[57]
J. Prendki,[57] L. Gladney,[58] M. Biasini,[59] R. Covarelli,[59] E. Manoni,[59] C. Angelini,[60] G. Batignani,[60] S. Bettarini,[60]
M. Carpinelli,[60, ¶] A. Cervelli,[60] F. Forti,[60] M. A. Giorgi,[60] A. Lusiani,[60] G. Marchiori,[60] M. Morganti,[60]
N. Neri,[60] E. Paoloni,[60] G. Rizzo,[60] J. J. Walsh,[60] J. Biesiada,[61] Y. P. Lau,[61] D. Lopes Pegna,[61] C. Lu,[61]
J. Olsen,[61] A. J. S. Smith,[61] A. V. Telnov,[61] E. Baracchini,[62] G. Cavoto,[62] D. del Re,[62] E. Di Marco,[62]
R. Faccini,[62] F. Ferrarotto,[62] F. Ferroni,[62] M. Gaspero,[62] P. D. Jackson,[62] M. A. Mazzoni,[62] S. Morganti,[62]
G. Piredda,[62] F. Polci,[62] F. Renga,[62] C. Voena,[62] M. Ebert,[63] T. Hartmann,[63] H. Schröder,[63] R. Waldi,[63]
T. Adye,[64] B. Franek,[64] E. O. Olaiya,[64] W. Roethel,[64] F. F. Wilson,[64] S. Emery,[65] M. Escalier,[65]
A. Gaidot,[65] S. F. Ganzhur,[65] G. Hamel de Monchenault,[65] W. Kozanecki,[65] G. Vasseur,[65] Ch. Yèche,[65]
M. Zito,[65] X. R. Chen,[66] H. Liu,[66] W. Park,[66] M. V. Purohit,[66] R. M. White,[66] J. R. Wilson,[66] M. T. Allen,[67]
D. Aston,[67] R. Bartoldus,[67] P. Bechtle,[67] J. F. Benitez,[67] R. Cenci,[67] J. P. Coleman,[67] M. R. Convery,[67]
J. C. Dingfelder,[67] J. Dorfan,[67] G. P. Dubois-Felsmann,[67] W. Dunwoodie,[67] R. C. Field,[67] T. Glanzman,[67]
S. J. Gowdy,[67] M. T. Graham,[67] P. Grenier,[67] C. Hast,[67] W. R. Innes,[67] J. Kaminski,[67] M. H. Kelsey,[67] H. Kim,[67]
P. Kim,[67] M. L. Kocian,[67] D. W. G. S. Leith,[67] S. Li,[67] B. Lindquist,[67] S. Luitz,[67] V. Luth,[67] H. L. Lynch,[67]
D. B. MacFarlane,[67] H. Marsiske,[67] R. Messner,[67] D. R. Muller,[67] H. Neal,[67] S. Nelson,[67] C. P. O'Grady,[67]
I. Ofte,[67] A. Perazzo,[67] M. Perl,[67] B. N. Ratcliff,[67] A. Roodman,[67] A. A. Salnikov,[67] R. H. Schindler,[67]
J. Schwiening,[67] A. Snyder,[67] D. Su,[67] M. K. Sullivan,[67] K. Suzuki,[67] S. K. Swain,[67] J. M. Thompson,[67]
J. Va'vra,[67] A. P. Wagner,[67] M. Weaver,[67] W. J. Wisniewski,[67] M. Wittgen,[67] D. H. Wright,[67] H. W. Wulsin,[67]
A. K. Yarritu,[67] K. Yi,[67] C. C. Young,[67] V. Ziegler,[67] P. R. Burchat,[68] A. J. Edwards,[68] S. A. Majewski,[68]
T. S. Miyashita,[68] B. A. Petersen,[68] L. Wilden,[68] S. Ahmed,[69] M. S. Alam,[69] R. Bula,[69] J. A. Ernst,[69] B. Pan,[69]
M. A. Saeed,[69] S. B. Zain,[69] S. M. Spanier,[70] B. J. Wogsland,[70] R. Eckmann,[71] J. L. Ritchie,[71] A. M. Ruland,[71]
C. J. Schilling,[71] R. F. Schwitters,[71] J. M. Izen,[72] X. C. Lou,[72] S. Ye,[72] F. Bianchi,[73] D. Gamba,[73]
M. Pelliccioni,[73] M. Bomben,[74] L. Bosisio,[74] C. Cartaro,[74] F. Cossutti,[74] G. Della Ricca,[74] L. Lanceri,[74]
L. Vitale,[74] V. Azzolini,[75] N. Lopez-March,[75] F. Martinez-Vidal,[75] D. A. Milanes,[75] A. Oyanguren,[75] J. Albert,[76]
Sw. Banerjee,[76] B. Bhuyan,[76] K. Hamano,[76] R. Kowalewski,[76] I. M. Nugent,[76] J. M. Roney,[76] R. J. Sobie,[76]
T. J. Gershon,[77] P. F. Harrison,[77] J. Ilic,[77] T. E. Latham,[77] G. B. Mohanty,[77] H. R. Band,[78] X. Chen,[78]
S. Dasu,[78] K. T. Flood,[78] P. E. Kutter,[78] Y. Pan,[78] M. Pierini,[78] R. Prepost,[78] C. O. Vuosalo,[78] and S. L. Wu[78]
(The *BABAR* Collaboration)

[1]*Laboratoire de Physique des Particules, IN2P3/CNRS et Université de Savoie, F-74941 Annecy-Le-Vieux, France*
[2]*Universitat de Barcelona, Facultat de Fisica, Departament ECM, E-08028 Barcelona, Spain*
[3]*Università di Bari, Dipartimento di Fisica and INFN, I-70126 Bari, Italy*
[4]*University of Bergen, Institute of Physics, N-5007 Bergen, Norway*
[5]*Lawrence Berkeley National Laboratory and University of California, Berkeley, California 94720, USA*
[6]*University of Birmingham, Birmingham, B15 2TT, United Kingdom*
[7]*Ruhr Universität Bochum, Institut für Experimentalphysik 1, D-44780 Bochum, Germany*
[8]*University of Bristol, Bristol BS8 1TL, United Kingdom*
[9]*University of British Columbia, Vancouver, British Columbia, Canada V6T 1Z1*
[10]*Brunel University, Uxbridge, Middlesex UB8 3PH, United Kingdom*
[11]*Budker Institute of Nuclear Physics, Novosibirsk 630090, Russia*
[12]*University of California at Irvine, Irvine, California 92697, USA*
[13]*University of California at Los Angeles, Los Angeles, California 90024, USA*
[14]*University of California at Riverside, Riverside, California 92521, USA*
[15]*University of California at San Diego, La Jolla, California 92093, USA*
[16]*University of California at Santa Barbara, Santa Barbara, California 93106, USA*
[17]*University of California at Santa Cruz, Institute for Particle Physics, Santa Cruz, California 95064, USA*
[18]*California Institute of Technology, Pasadena, California 91125, USA*
[19]*University of Cincinnati, Cincinnati, Ohio 45221, USA*
[20]*University of Colorado, Boulder, Colorado 80309, USA*
[21]*Colorado State University, Fort Collins, Colorado 80523, USA*
[22]*Universität Dortmund, Institut für Physik, D-44221 Dortmund, Germany*
[23]*Technische Universität Dresden, Institut für Kern- und Teilchenphysik, D-01062 Dresden, Germany*
[24]*Laboratoire Leprince-Ringuet, CNRS/IN2P3, Ecole Polytechnique, F-91128 Palaiseau, France*
[25]*University of Edinburgh, Edinburgh EH9 3JZ, United Kingdom*
[26]*Università di Ferrara, Dipartimento di Fisica and INFN, I-44100 Ferrara, Italy*
[27]*Laboratori Nazionali di Frascati dell'INFN, I-00044 Frascati, Italy*
[28]*Università di Genova, Dipartimento di Fisica and INFN, I-16146 Genova, Italy*
[29]*Harvard University, Cambridge, Massachusetts 02138, USA*
[30]*Universität Heidelberg, Physikalisches Institut, Philosophenweg 12, D-69120 Heidelberg, Germany*

[31]*Imperial College London, London, SW7 2AZ, United Kingdom*
[32]*University of Iowa, Iowa City, Iowa 52242, USA*
[33]*Iowa State University, Ames, Iowa 50011-3160, USA*
[34]*Johns Hopkins University, Baltimore, Maryland 21218, USA*
[35]*Universität Karlsruhe, Institut für Experimentelle Kernphysik, D-76021 Karlsruhe, Germany*
[36]*Laboratoire de l'Accélérateur Linéaire, IN2P3/CNRS et Université Paris-Sud 11,*
Centre Scientifique d'Orsay, B. P. 34, F-91898 ORSAY Cedex, France
[37]*Lawrence Livermore National Laboratory, Livermore, California 94550, USA*
[38]*University of Liverpool, Liverpool L69 7ZE, United Kingdom*
[39]*Queen Mary, University of London, E1 4NS, United Kingdom*
[40]*University of London, Royal Holloway and Bedford New College, Egham, Surrey TW20 0EX, United Kingdom*
[41]*University of Louisville, Louisville, Kentucky 40292, USA*
[42]*University of Manchester, Manchester M13 9PL, United Kingdom*
[43]*University of Maryland, College Park, Maryland 20742, USA*
[44]*University of Massachusetts, Amherst, Massachusetts 01003, USA*
[45]*Massachusetts Institute of Technology, Laboratory for Nuclear Science, Cambridge, Massachusetts 02139, USA*
[46]*McGill University, Montréal, Québec, Canada H3A 2T8*
[47]*Università di Milano, Dipartimento di Fisica and INFN, I-20133 Milano, Italy*
[48]*University of Mississippi, University, Mississippi 38677, USA*
[49]*Université de Montréal, Physique des Particules, Montréal, Québec, Canada H3C 3J7*
[50]*Mount Holyoke College, South Hadley, Massachusetts 01075, USA*
[51]*Università di Napoli Federico II, Dipartimento di Scienze Fisiche and INFN, I-80126, Napoli, Italy*
[52]*NIKHEF, National Institute for Nuclear Physics and High Energy Physics, NL-1009 DB Amsterdam, The Netherlands*
[53]*University of Notre Dame, Notre Dame, Indiana 46556, USA*
[54]*Ohio State University, Columbus, Ohio 43210, USA*
[55]*University of Oregon, Eugene, Oregon 97403, USA*
[56]*Università di Padova, Dipartimento di Fisica and INFN, I-35131 Padova, Italy*
[57]*Laboratoire de Physique Nucléaire et de Hautes Energies,*
IN2P3/CNRS, Université Pierre et Marie Curie-Paris6,
Université Denis Diderot-Paris7, F-75252 Paris, France
[58]*University of Pennsylvania, Philadelphia, Pennsylvania 19104, USA*
[59]*Università di Perugia, Dipartimento di Fisica and INFN, I-06100 Perugia, Italy*
[60]*Università di Pisa, Dipartimento di Fisica, Scuola Normale Superiore and INFN, I-56127 Pisa, Italy*
[61]*Princeton University, Princeton, New Jersey 08544, USA*
[62]*Università di Roma La Sapienza, Dipartimento di Fisica and INFN, I-00185 Roma, Italy*
[63]*Universität Rostock, D-18051 Rostock, Germany*
[64]*Rutherford Appleton Laboratory, Chilton, Didcot, Oxon, OX11 0QX, United Kingdom*
[65]*DSM/Dapnia, CEA/Saclay, F-91191 Gif-sur-Yvette, France*
[66]*University of South Carolina, Columbia, South Carolina 29208, USA*
[67]*Stanford Linear Accelerator Center, Stanford, California 94309, USA*
[68]*Stanford University, Stanford, California 94305-4060, USA*
[69]*State University of New York, Albany, New York 12222, USA*
[70]*University of Tennessee, Knoxville, Tennessee 37996, USA*
[71]*University of Texas at Austin, Austin, Texas 78712, USA*
[72]*University of Texas at Dallas, Richardson, Texas 75083, USA*
[73]*Università di Torino, Dipartimento di Fisica Sperimentale and INFN, I-10125 Torino, Italy*
[74]*Università di Trieste, Dipartimento di Fisica and INFN, I-34127 Trieste, Italy*
[75]*IFIC, Universitat de Valencia-CSIC, E-46071 Valencia, Spain*
[76]*University of Victoria, Victoria, British Columbia, Canada V8W 3P6*
[77]*Department of Physics, University of Warwick, Coventry CV4 7AL, United Kingdom*
[78]*University of Wisconsin, Madison, Wisconsin 53706, USA*

(Dated: May 30, 2008)

We perform a measurement of the *CP* asymmetry in $b \to s\gamma$ decays using a sample of 383×10^6 $B\overline{B}$ events collected by the *BABAR* detector at the PEP-II asymmetric B factory. We reconstruct sixteen flavor-specific B decay modes containing a high-energy photon and a hadronic system X_s containing an s quark. We measure the *CP* asymmetry to be $-0.011 \pm 0.030(\mathrm{stat}) \pm 0.014(\mathrm{syst})$ for a photon energy threshold at 1.6 GeV and the hadronic system mass between 0.6 and 2.8 GeV/c^2.

PACS numbers: 13.20.-v, 13.25.Hw

---

[*] Deceased

[†] Now at Temple University, Philadelphia, Pennsylvania 19122,

The decay $b \to s\gamma$ is a flavor-changing neutral current process described by a radiative penguin diagram in the Standard Model (SM). It is sensitive to new physics which can appear in branching fraction or *CP* asymmetry measurements. Recent experimental measurements of the branching fraction [1, 2] are in good agreement with SM predictions [3].

A *CP* asymmetry between $b \to s\gamma$ and $\bar{b} \to \bar{s}\gamma$ decays is predicted by the SM to be small ($\leq 1\%$) [4] but could be enhanced up to 15% [5, 6, 7] in models of physics beyond the SM. Published experimental results are all consistent with zero *CP* asymmetry, with a precision of 5% [8, 9]. The increased experimental precision obtained by the measurement presented in this work allows us to discriminate between various theoretical models [10].

We use a sample of 383×10^6 $B\overline{B}$ pairs collected at the $\Upsilon(4S)$ resonance with the PEP-II B factory. An additional $36.3\,\mathrm{fb}^{-1}$ of off-resonance data, taken at the center-of-mass (CM) energy 40 MeV below the $\Upsilon(4S)$ resonance, is used to study the background from non-B decays.

A detailed description of the BABAR detector can be found elsewhere [11]. Charged particles and their momenta are reconstructed from tracks measured with a five-layer silicon vertex tracker and a 40-layer drift chamber inside a 1.5-T solenoidal magnet. An electromagnetic calorimeter (EMC) consisting of 6580 CsI(Tl) crystals is used to identify electrons and photons. A ring-imaging Cherenkov detector (DIRC) is used to separate charged pions from kaons. Resistive-plate chambers and limited streamer tubes embedded in the flux return of the solenoid are used to identify muons.

We reconstruct 16 exclusive $b \to s\gamma$ final states:

$$\begin{aligned}
B^- \;\to\;& K^0_S\pi^-\gamma, K^-\pi^0\gamma, K^-\pi^+\pi^-\gamma, K^0_S\pi^-\pi^0\gamma,\\
& K^-\pi^0\pi^0\gamma, K^0_S\pi^+\pi^-\pi^-\gamma, K^-\pi^+\pi^-\pi^0\gamma,\\
& K^0_S\pi^-\pi^0\pi^0\gamma, K^-\eta\gamma, K^+K^-K^-\gamma,\\
\overline{B}^0 \;\to\;& K^-\pi^+\gamma, K^-\pi^+\pi^0\gamma, K^-\pi^+\pi^-\pi^+\gamma, K^-\pi^+\pi^0\pi^0\gamma,\\
& K^-\pi^+\eta\gamma, K^+K^-K^-\pi^+\gamma
\end{aligned}$$

and measure the yield asymmetry with respect to their charge conjugate decays $\bar{b} \to \bar{s}\gamma$. These modes are selected because the particles in the final state identify the flavor of the B meson and they can be reconstructed with high statistical significance.

The hadronic system X_s, formed from the kaons and pions, is required to have an invariant mass M_{X_s} between 0.6 and 2.8 GeV/c^2 corresponding to a photon energy threshold $E_\gamma > 1.90$ GeV in the B meson rest frame.

The high-energy photon from the B decay is reconstructed from an isolated energy cluster in the calorimeter, with a shape consistent with the electromagnetic shower produced by a single photon and an energy $E^*_\gamma >$ 1.6 GeV in the $\Upsilon(4S)$ CM frame.

Charged kaons are identified by combining information from the DIRC and the energy-loss measurements from the tracking system. The remaining tracks are considered to be charged pions. The K^0_S candidates are reconstructed by combining two oppositely charged pions. These two pions are required to have an invariant mass within 9 MeV/c^2 of the nominal K^0_S mass [12] and a minimum flight distance of 2 mm from the primary event vertex. Both charged and neutral kaons are required to have a laboratory momenta greater than 800 MeV/c.

Neutral pions are reconstructed from pairs of photons with energies above 50 MeV in the laboratory frame, and a lateral moment [13] less than 0.8. Cutting on the lateral moment, a measure of the spread of a shower in the EMC, gives good separation between electromagnetic and hadronic showers. The π^0 candidate mass is required to be between 115 and 150 MeV/c^2. Charged and neutral pions are required to have laboratory momenta greater than 200 MeV/c.

We reconstruct η candidates by combining two photons, each with an energy above 50 MeV in the laboratory reference frame, and a lateral moment less than 0.8. The η candidates are required to have laboratory momenta greater than 200 MeV/c, and their invariant masses are required to be between 470 and 620 MeV/c^2.

Monte Carlo (MC) samples based on EvtGen [14] and GEANT4 [15] are used to simulate the signal and background processes and the detector response. The $b \to s\gamma$ signal sample is generated with a photon spectrum derived from Ref.[4] assuming $m_b = 4.65\,\mathrm{GeV}/c^2$. JETSET [16] is used to model the fragmentation of the X_s system in the signal MC. We correct it using the BABAR-measured fragmentation as described later.

The background to the B reconstruction is dominated by continuum processes ($e^+e^- \to q\bar{q}$, with $q = u, d, s, c$) that produce a high-energy photon either by initial-state radiation or from the decay of π^0 and η mesons. Continuum events tend to be less isotropic than B-decay events since they result from hadronic fragmentation of high-momentum quarks back-to-back in the CM frame. High-energy photons in these events tend to be collinear with the thrust axis formed from the rest of the event (ROE), defined as those particles not used in reconstructing the signal B candidate. We reject such backgrounds by requiring that the cosine of the angle between the photon and the thrust axis of the ROE (in the CM frame) be less than 0.85. We further reject the continuum events by requiring the ratio of the second (L_2) and zeroth (L_0) Legendre moments for the ROE particles with respect to the B flight direction of the event to be smaller than 0.46. This is because the continuum events tend to have most of the decay particles momenta aligned closely with the ROE thrust axis, thus leading to larger values of L_2/L_0

USA

[‡] Now at Tel Aviv University, Tel Aviv, 69978, Israel

[§] Also with Università di Perugia, Dipartimento di Fisica, Perugia, Italy

[¶] Also with Universita' di Sassari, Sassari, Italy than the signal events.

Continuum events with high-energy photons from π^0 and η decay are major backgrounds. In order to veto those events, we associate each high-energy photon candidate γ with another photon candidate γ' in the event. For multiple γ' candidate in an event, we choose the $\gamma\gamma'$ pairs whose invariant mass, determined from simply adding the four vectors, is closest to the nominal π^0 mass (or η mass in case of η veto). Events are rejected if the photon pairs are consistent with π^0 or η decays based on the output of a boosted decision tree (BDT) [17] constructed from the energy of the less energetic photon γ' and $m_{\gamma\gamma'}$.

We reject the remaining continuum events by constructing an additional BDT that combines information from a number of variables related to the event shape, the kinematic properties of the B meson, and the flavor-tagging [18] properties of the other B meson in the event. Examples of these variables are the Fox-Wolfram moments [19], and the cosine of the B flight direction computed in the CM frame with respect to the beam axis. Optimization of the selection criteria of the π^0 veto, η veto, and event selection BDTs is performed using an iterative method which maximizes the statistical signal significance. After the final event selection, we find that we reject 97% of the continuum background while retaining 55% of the signal events.

Fully reconstructed $b \to s\gamma$ decays are characterized by two kinematic variables: the beam-energy substituted mass $m_{\rm ES} = \sqrt{s/4 - {p_B^*}^2}$, and the energy difference between the B candidate and the beam energy $\Delta E = E_B^* - \sqrt{s}/2$, where E_B^* and p_B^* are the energy and momentum of the B candidate in the e^+e^- CM frame, and $\sqrt{s}$ is the total CM frame energy. Signal events are expected to have a ΔE distribution centered near zero and a $m_{\rm ES}$ distribution centered at the mass of the B meson. For events with multiple B candidates, we select the one with the smallest $|\Delta E|$.

We perform a one-dimensional fit of $m_{\rm ES}$ to the data in five different regions of M_{X_s}: [0.6, 1.1], [1.1, 1.5], [1.5, 2.0] and [2.0, 2.8] GeV/c^2, as well as the entire M_{X_s} region [0.6, 2.8] GeV/c^2 to study whether the asymmetry has significant mass dependence. Only candidates in the range $|\Delta E| < 0.10\,{\rm GeV}$ and $5.22 < m_{\rm ES} < 5.29\,{\rm GeV}/c^2$ are considered. Probability density functions (PDFs) are constructed for both signal and background in the five M_{X_s} regions. We use the charge of the reconstructed final state (B^-/B^+) or the charge of the kaon ($\overline{B}^0/B^0$) to define two flavor categories, and perform a simultaneous fit for the flavor asymmetry in each M_{X_s} region.

The signal events are described by a function $f(m_{\rm ES}) = \exp[-(m_{\rm ES}-\mu_0)^2/(2\sigma_{L,R}^2+\alpha_{L,R}(m_{\rm ES}-\mu_0)^2)]$ where the parameters are determined by an unbinned fit to the signal MC. In the above function, μ_0 is the peak position of the distribution, $\sigma_{L,R}$ are the widths on the left and right of the peak, and $\alpha_{L,R}$ parameterize the tail on the left and right of the peak, respectively.

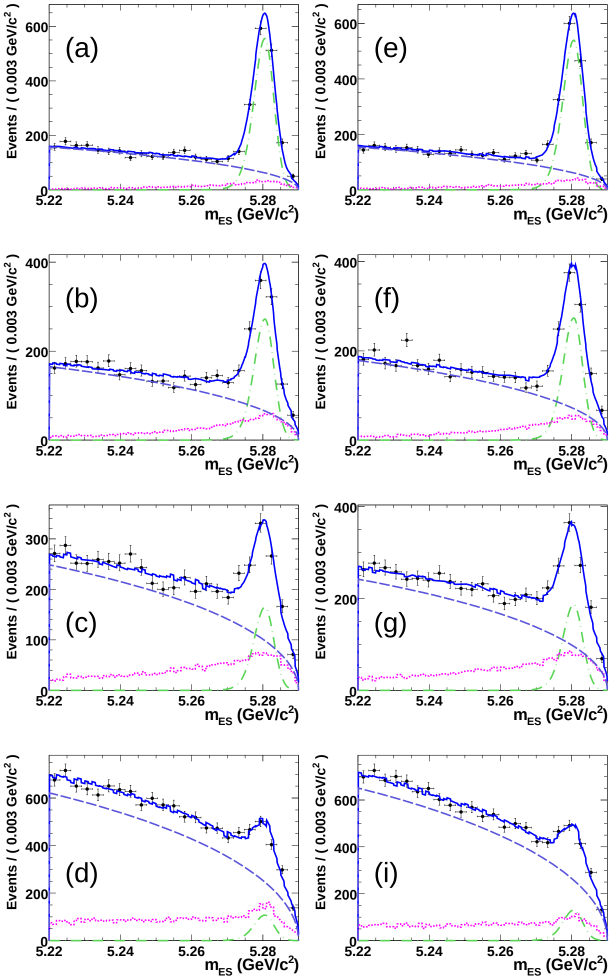

FIG. 1: Fits to the $m_{\rm ES}$ distribution in data for $b \to s\gamma$ events in M_{X_s} region (a) [0.6, 1.1], (b) [1.1, 1.5], (c) [1.5, 2.0], (d) [2.0, 2.8], and $\bar{b} \to \bar{s}\gamma$ events in M_{X_s} region (e) [0.6, 1.1], (f) [1.1, 1.5], (g) [1.5, 2.0], (h) [2.0, 2.8], The dashed line shows the shape of the continuum, dotted-dashed line shows the fitted signal shape and the dotted line shows the $B\overline{B}$ and cross-feed shape.

The background surviving the final selection can be attributed to one of three sources: continuum events, $B\overline{B}$ events other than $b \to s\gamma$ decays, (referred to as generic $B\overline{B}$ in the following), and "cross-feed events", defined as events containing a $b \to s\gamma$ decay, but in which the true $b \to s\gamma$ decay was not correctly reconstructed. The shape of the cross-feed background together with the $B\overline{B}$ background is described by a binned PDF, determined from MC with 1 MeV/c^2 binning.

The continuum background is described by an ARGUS function [20] determined from a fit to the off-resonance data. In this fit, the $m_{\rm ES}$ distribution is shifted to have the same end-point as that of the on-resonance data.

In the maximum-likelihood (ML) fit, all parameters are fixed with the exception of μ_0, which is determined from fitting the data, since the peak position is not well mod-

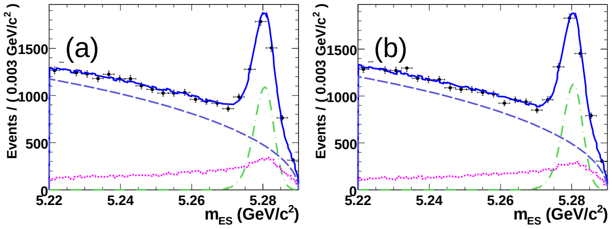

FIG. 2: Fits to the $m_{\rm ES}$ distribution in data for (a) $b \to s\gamma$ events in and (b) $\bar{b} \to \bar{s}\gamma$ events in the entire M_{X_s} region. The dashed line shows the shape of the continuum, dotted-dashed line shows the fitted signal shape and the dotted line shows the $B\overline{B}$ and cross-feed shape.

eled in the MC simulation. The signal, $B\overline{B}$ and cross-feed shape are constrained by the MC, while the continuum background shape is fixed to the off-resonance data shape. The shapes of the distributions are assumed to be the same for B and $\overline{B}$ candidates, with the exception of the $B\overline{B}$ and cross-feed background, which are allowed to vary between b and $\bar{b}$ in order to eliminate the possibility of a false *CP* asymmetry. In Figure 1 we present the final fits to the $m_{\rm ES}$ distributions for $b \to s\gamma$ and $\bar{b} \to \bar{s}\gamma$ events for the four M_{X_s} sub-regions. We observe a significant drop of the signal to background ratio from lower to higher M_{X_s} regions. In Figure 2, we present the final fits to the $m_{\rm ES}$ distribution for $b \to s\gamma$ and $\bar{b} \to \bar{s}\gamma$ events for the entire M_{X_s} region.

The direct *CP* asymmetry is calculated as

$$A_{CP} = \frac{1}{\langle D \rangle}\left(\frac{N_b - N_{\overline{b}}}{N_b + N_{\overline{b}}} - \Delta D\right) - A_{det} \qquad (1)$$

where N_b and $N_{\overline{b}}$ are the yields of the $b \to s\gamma$ and $\bar{b} \to \bar{s}\gamma$ signals respectively. We assume the same selection efficiency for each mode. A_{det}, described in details below, is the flavor bias caused by the detector responses to positively and negatively charged particles. Table I presents the fitted values for $(N_b - N_{\overline{b}})/(N_b + N_{\overline{b}})$.

$\Delta D = (\bar{\omega} - \omega)$ is the difference in the wrong-flavor fraction between b and $\bar{b}$ decays, and $\langle D \rangle = 1 - (\bar{\omega} + \omega)$ is the dilution factor from the average wrong-flavor fraction. The small wrong-flavor fraction $\bar{\omega}$ (ω), defined to be the fraction of $\bar{b}$ (b) reconstructed as the opposite flavor, is due to charged pions misidentified as charged kaons. We evaluate it using the particle misidentification rate measured in control samples from the data. We find $\Delta D = (5 \pm 4) \times 10^{-5}$ and $1 - \langle D \rangle = (5.4 \pm 0.1) \times 10^{-3}$, which are negligibly small.

The flavor bias of the detector A_{det} is due to asymmetric K^+, K^- interaction cross-sections in the detector at low momenta. Such an asymmetry could produce a false *CP* asymmetry in the signal events. We perform a measurement of A_{det} in data using two independent methods. The first approach is to determine this asymmetry from events in the $m_{\rm ES}$ sideband, $5.22 < m_{\rm ES} < 5.27\,{\rm GeV}/c^2$, which is dominated by continuum background with no expected *CP* asymmetry. The second approach is to construct a control sample where we replace the high-energy photon from the B decay with a high-energy π^0, with a minimum CM momentum of $1.6\,{\rm GeV}/c$. We apply all selection criteria identically to our signal selection, except that we remove the π^0 and η veto requirements, and again measure the *CP* asymmetry in the $m_{\rm ES}$ sideband. In both of these control samples, we apply appropriate weights to the events to ensure that the fraction of each reconstructed final state is identical to that in the signal sample. We find the *CP* asymmetry measured using both of these approaches to be nearly identical: -0.006 ± 0.006 (signal sideband) and -0.007 ± 0.007 (control sample sideband) and average them to obtain $A_{det} = -0.007 \pm 0.005$. Its mean values are used to shift $(N_b - N_{\overline{b}})/(N_b + N_{\overline{b}})$ mean value, while the errors are propagated in the systematic errors. We also calculate A_{det} for each X_s mass region (Table I).

The shape of the $B\overline{B}$ and cross-feed background, determined from MC, could also be a potential source of flavor bias in the fit to the data. This background peaks broadly in the signal region, and a small shape difference as a function of flavor could create a false *CP* asymmetry in the signal events. We measure the size of this effect by correcting the $B\overline{B}$ and cross-feed shapes separately. The high-energy π^0 control sample mentioned above is used to study the uncertainty of the $B\overline{B}$ background shape. We use the differences found between the data and MC $m_{\rm ES}$ shapes in this control sample to correct the nominal $B\overline{B}$ background shape built from the MC. The biggest uncertainty in the cross-feed shape is due to the fact that JETSET does not reproduce the observed fragmentation structure of data. We thus correct the simulation shape using the fragmentation previously determined from *BABAR* data in Ref. [21]. We then construct new b and $\bar{b}$ binned PDFs using these corrected cross-feed and $B\overline{B}$ events and fit the data a second time with them. The difference between the nominal A_{CP} and A_{CP} from this fit, shown in Table I, is used as the systematic error from shape modeling of the B background.

The systematic error arising from the continuum background modeling is determined by varying the ARGUS shape parameters within the experimental errors. The effect on A_{CP} from this variation is found to be 0.006 for the combined M_{X_s} region, shown in Table I.

We have checked that the signal shape is the same for b and $\bar{b}$ events, and the effect on A_{CP} by varying the signal shape is minimal: -0.018% which is beyond the sensitivity of this analysis. The dominant systematic errors in our measurement are therefore the uncertainties in the flavor bias of the detector and the background shapes as described above. Total systematic errors are calculated as the sum in quadrature of errors on A_{det}, systematic errors arising from the continuum, $B\overline{B}$ and cross-feed shape modeling. Contributions from $\langle D \rangle$, ΔD and signal modeling are neglected due to the small impact on A_{CP}. The results as a spectrum of M_{X_s} are shown in

M_{Xs} (GeV/c^2)	$\frac{N_b - N_{\overline{b}}}{N_b + N_{\overline{b}}}$	A_{det}	$B\overline{B}$ and cross-feed model syst	Continuum model syst	A_{CP}
0.6–1.1	0.015 ± 0.029	0.005 ± 0.014	0.002	0.004	$0.010 \pm 0.029 \pm 0.015$
1.1–1.5	-0.003 ± 0.049	-0.003 ± 0.015	0.003	0.004	$0.000 \pm 0.049 \pm 0.016$
1.5–2.0	-0.064 ± 0.077	-0.017 ± 0.010	0.010	0.002	$-0.047 \pm 0.077 \pm 0.014$
2.0–2.8	-0.097 ± 0.180	-0.002 ± 0.005	0.070	0.168	$-0.077 \pm 0.180 \pm 0.182$
0.6–2.8	-0.018 ± 0.030	-0.007 ± 0.005	0.012	0.006	$-0.011 \pm 0.030 \pm 0.014$

TABLE I: For each M_{X_s} bin, we present the fitted *CP* asymmetry: $(N_b - N_{\overline{b}})/(N_b + N_{\overline{b}})$, the flavor-bias of the detector: A_{det}, the systematic error arising from the $B\overline{B}$ and cross-feed modeling and the systematic error arising from the continuum background modeling. The last column shows the final results for the *CP* asymmetries.

Table I.

In summary, we measure the direct *CP* asymmetry in $b \to s\gamma$ to be $A_{CP} = -0.011 \pm 0.030 \pm 0.014$ in the region $0.6 < M_{X_s} < 2.8\,\mathrm{GeV}/c^2$. This is the most accurate measurement of this quantity to date. It is consistent with zero *CP* asymmetry and the SM prediction. The *CP* asymmetry in each M_{X_s} region under our study is also consistent with zero.

We are grateful for the excellent luminosity and machine conditions provided by our PEP-II colleagues, and for the substantial dedicated effort from the computing organizations that support *BABAR*. The collaborating institutions wish to thank SLAC for its support and kind hospitality. This work is supported by DOE and NSF (USA), NSERC (Canada), CEA and CNRS-IN2P3 (France), BMBF and DFG (Germany), INFN (Italy), FOM (The Netherlands), NFR (Norway), MES (Russia), MEC (Spain), and STFC (United Kingdom). Individuals have received support from the Marie Curie EIF (European Union) and the A. P. Sloan Foundation.

[1] *BABAR* Collaboration, B. Aubert *et al.*, Phys. Rev. **D72**, 052004 (2005).
[2] *BABAR* Collaboration, B. Aubert *et al.*, Phys. Rev. Lett. **97**, 171803 (2006).
[3] M. Misiak et al., Phys. Rev. Lett. **98**, 022002 (2007).
[4] A. L. Kagan and M. Neubert, Phys. Rev. **D58**, 094012 (1998).
[5] L. Wolfenstein and Y. L. Wu, Phys. Rev. Lett. **73**, 2809 (1994).
[6] G. M. Asatrian and A. Ioannisian, Phys. Rev. **D54**, 5642 (1996).
[7] M. Ciuchini, E. Gabrielli, and G. F. Giudice, Phys. Lett. **B388**, 353 (1996).
[8] *BABAR* Collaboration, B. Aubert *et al.*, Phys. Rev. Lett. **93**, 021804 (2004).
[9] Belle Collaboration, Nishida, S. *et al.*, Phys. Rev. Lett. **93**, 031803 (2004).
[10] T. Hurth, E. Lunghi, and W. Porod, Nucl. Phys. **B704**, 56 (2005).
[11] *BABAR* Collaboration, B. Aubert *et al.*, Nucl. Instrum. Methods **A479**, 1 (2002).
[12] W. M. Yao et al. (Particle Data Group), J. Phys. **G33**, 1 (2006).
[13] A. Drescher et al., Nucl. Instrum. Meth. **A237**, 464 (1985).
[14] D. J. Lange, Nucl. Instrum. Meth. **A462**, 152 (2001).
[15] GEANT4 Collaboration, S. Agostinelli *et al.*, Nucl. Instrum. Methods **A506**, 250 (2003).
[16] T. Sjostrand, Computer Phys. Commun. **82**, 74 (1994).
[17] I. Narsky and J. Bunn, Proceedings of Computing for High Energy Physics, Mumbai, India, February 13-17 (2006).
[18] *BABAR* Collaboration, B. Aubert *et al.*, Phys. Rev. Lett. **89**, 201802 (2002).
[19] G. C. Fox and S. Wolfram, Phys. Rev. Lett. **41**, 1581 (1978).
[20] ARGUS Collaboration, Albrecht, H. *el al.*, Phys. Lett. **B185**, 218 (1987).
[21] *BABAR* Collaboration, B. Aubert *et al.*, Phys. Rev. **D72**, 052004 (2005).